



Cold dilute nuclear matter with α -particle condensation in a generalized nonlinear relativistic mean-field model

Zhao-Wen Zhang and Lie-Wen Chen ^{*}

*School of Physics and Astronomy and Shanghai Key Laboratory for Particle Physics and Cosmology,
Shanghai Jiao Tong University, Shanghai 200240, China*

 (Received 12 March 2019; revised manuscript received 25 August 2019; published 4 November 2019)

We explore the thermodynamic properties of homogeneous cold (zero-temperature) nuclear matter including nucleons and α -particle condensation at low densities by using a generalized nonlinear relativistic mean-field (gNL-RMF) model. In the gNL-RMF model, the α particle is included as an explicit degree of freedom and treated as a pointlike particle with its interaction described by meson exchanges, and the in-medium effects on the α binding energy are described by density- and temperature-dependent energy shift with the parameters obtained by fitting the experimental Mott density. We find that below the dropping density $n_{\text{drop}} (\approx 3 \times 10^{-3} \text{ fm}^{-3})$, the zero-temperature symmetric nuclear matter is in the state of pure Bose-Einstein condensate (BEC) of α particles while the neutron-rich nuclear matter is composed of α -BEC and neutrons. Above the n_{drop} , the fraction of α -BEC decreases with density and vanishes at the transition density $n_t (\approx 8 \times 10^{-3} \text{ fm}^{-3})$. Above the n_t , the nuclear matter becomes pure nucleonic matter. Our results indicate that the empirical parabolic law for the isospin asymmetry dependence of the nuclear matter equation of state is heavily violated by the α -particle condensation in the zero-temperature dilute nuclear matter, making the conventional definition of the symmetry energy meaningless. We investigate the symmetry energy defined under parabolic approximation for the zero-temperature dilute nuclear matter with α -particle condensation and find it is significantly enhanced compared to the case without clusters and becomes saturated at about 7 MeV at very low densities ($\lesssim 10^{-3} \text{ fm}^{-3}$). The critical temperature for α condensation in homogeneous dilute nuclear matter is also discussed.

DOI: [10.1103/PhysRevC.100.054304](https://doi.org/10.1103/PhysRevC.100.054304)

I. INTRODUCTION

The investigation of clustering effects in nuclear matter and finite nuclei is currently a hot topic in nuclear physics. It is known that the nuclear matter system can minimize its energy by forming light clusters at very low densities [1–5]. The clustering phenomenon may exist in various nuclear and astrophysical processes or objects, such as nuclear ground states and excited states [6–11], heavy-ion collisions [12–17], core-collapse supernovae [18,19], and the crust of neutron stars [20–24]. The light clusters such as deuterons ($d = {}^2\text{H}$), tritons ($t = {}^3\text{H}$), helium-3 ($h = {}^3\text{He}$), and α particles ($\alpha = {}^4\text{He}$) will become unbound in nuclear matter when the density is larger than a critical density, i.e., the Mott density. Therefore, the clustering effects is important for understanding the properties of nuclear matter, e.g., the nuclear matter equation of state (EOS), at low densities, especially below the Mott density. Since the deuterons and α particles are bosons, the Bose-Einstein condensation of d and α particles may occur in dilute nuclear matter systems when the temperature is lower than the corresponding critical temperature, and the resulting Bose-Einstein condensate (BEC) may play an important role in understanding the properties of the dilute nuclear matter system.

There have a large number of works devoted to the exploration of clustering effects in various nuclear and astrophysical systems. Of particular interest is the α -clustering phenomenon, due to the especially stable structure of α particles. In recent decades, great efforts have been made to study the properties of self-conjugate $4N$ nuclei (e.g., ${}^{12}\text{C}$ and ${}^{16}\text{O}$) in order to understand the condensation of α particles in finite nuclei [25–31]. The formation of α particles in the nuclear surface region of heavy nuclei is investigated by Typel [32,33]. In particular, a Wentzel-Kramers-Brillouin (WKB) approximation is used to obtain the α -particle wave function self-consistently with the nucleon distributions in the finite nuclei at zero temperature. In addition, during the past decades, the α -clustering effects have also been widely investigated in nuclear matter and compact stars [34–38]. In the Lattimer-Swesty EOS constructed by Lattimer and Swesty [39] and the Shen EOS constructed by Shen *et al.* [40], the α particles are included and treated as an ideal Boltzmann gas. Typel *et al.* studied the nuclear matter including formation of light clusters up to the α particle with a generalized density-dependent relativistic mean-field (gDD-RMF) model [2]. The EOS of dilute nuclear matter including nucleons and α particles at finite temperatures is also explored by using the virial expansion [41], and later on the additional contributions from d , t , and h as well as heavier nuclei are further included by using the S -matrix method and the quasiparticle gas model [42–44]. Ferreira and Provindência [45] explored the effect

^{*}Corresponding author: lwchen@sjtu.edu.cn

of the cluster-meson coupling constants on the dissolution density. They used theoretical and experimental constraints to fix the cluster-meson couplings and obtain the relative fractions of light clusters at finite temperature. Furthermore, Pais *et al.* investigated the effects of the cluster-meson coupling constants on the properties of warm stellar matter [46] and asymmetric warm nuclear matter [47]. In addition, the thermodynamic stability, phase coexistence, and phase transition in dilute nuclear matter including light nuclei were investigated in Refs. [2,22–24].

Furthermore, Mişicu *et al.* [48] investigated the behavior of boson complex scalar fields associated with α particles and anti- α particles by using the relativistic mean-field (RMF) method. They considered both compressed standard baryonic matter with small admixtures of α particles and systems comprising α particles that are gradually doped with symmetric nuclear matter, and calculated the energy of the momentum $\mathbf{k} = 0$ state, which can be viewed as the BEC of α matter. Using the momentum-projected Hartree-Fock approximation, Röpke *et al.* [49–51] calculated the critical temperature of α condensation in dilute nuclear matter.

In our previous work [52], a generalized nonlinear relativistic mean-field (gNL-RMF) model was developed to describe the low-density nuclear matter including nucleons, d , t , h , and α particles at finite temperature. It was found that the clustering effect may significantly influence the EOS of nuclear matter at low densities ($\lesssim 0.02 \text{ fm}^{-3}$). The temperature considered in Ref. [52] was above 3 MeV, and the α condensation was ignored there since it cannot occur at the considered temperature region in the gNL-RMF model. Given that more stringent constraints on the EOS of zero-temperature asymmetric nuclear matter, especially the zero-temperature symmetry energy, at subsaturation densities, have been obtained from theoretical model analyses on nuclear experimental data (see, e.g., Ref. [53]), it is thus very interesting to investigate the α condensation and its influence on the low-density behaviors of the EOS of zero-temperature asymmetric nuclear matter and the symmetry energy at zero temperature, which provides the main motivation of the present work.

In this work, we explore the properties of cold (zero-temperature) dilute nuclear matter using the gNL-RMF model. At zero temperature, the dilute nuclear matter is composed of nucleons and α -BEC. The existence of the α -BEC is shown to violate the empirical parabolic law for the isospin asymmetry dependence of nuclear matter EOS and makes the conventional definition of the symmetry energy meaningless. The symmetry energy defined under parabolic approximation displays a significant enhancement compared to the case without clusters and is found to be saturated at about 7 MeV at very low densities ($\lesssim 10^{-3} \text{ fm}^{-3}$).

This paper is organized as follows. In Sec. II, we introduce the gNL-RMF model for low-density nuclear matter including nucleons and α particles, and then the theoretical results and discussions are presented in Sec. III. Finally, we give a conclusion in Sec. IV.

II. THEORETICAL FRAMEWORK

In the nonlinear RMF (NL-RMF) model [54–61], the nonlinear couplings of mesons are introduced to reproduce

the ground-state properties of finite nuclei and to modify the density dependence of the symmetry energy. The gNL-RMF model [52] is an extension of the NL-RMF model including additional light nuclei degrees of freedom, i.e., d , t , h , and α particles. The light nuclei are treated as pointlike particles and they interact via the exchange of various effective mesons such as isoscalar scalar (σ) and vector (ω) mesons and an isovector vector (ρ) meson. The in-medium effect on the binding energy of light nuclei is described by density- and temperature-dependent energy shift, and the parameters of binding energy shift are determined by fitting the Mott density extracted from the experimental data [62] (see Ref. [52] for the details).

As the temperature decreases, the light nuclei except the α particles make decreasing contributions to the dilute nuclear matter system. Our calculations indicate that the contributions of d , t , and h can be neglected at extremely low temperatures, i.e., below about 1 MeV. The fractions of d , t , and h , which are defined by $Y_d = 2n_d/n_{\text{tot}}$, $Y_t = 3n_t/n_{\text{tot}}$, and $Y_h = 3n_h/n_{\text{tot}}$, respectively, are smaller than about 10^{-5} at such extremely low temperatures. Therefore, the light nuclei d , t , and h are not taken into account in the present gNL-RMF model calculations for the zero-temperature dilute nuclear matter. The Lagrangian density of the homogeneous nuclear matter system including nucleons, α particles, and mesons reads

$$\mathcal{L} = \sum_{i=p,n} \mathcal{L}_i + \mathcal{L}_\alpha + \mathcal{L}_{\text{meson}}, \quad (1)$$

where the nucleons ($i = p, n$) with spin 1/2 are described by

$$\mathcal{L}_i = \bar{\Psi}_i [\gamma_\mu iD_i^\mu - M_i^*] \Psi_i, \quad (2)$$

while the Lagrangian density of α particles with spin 0 is given by

$$\mathcal{L}_\alpha = \frac{1}{2} (iD_\alpha^\mu \phi_\alpha)^* (iD_{\mu\alpha} \phi_\alpha) - \frac{1}{2} \phi_\alpha^* (M_\alpha^*)^2 \phi_\alpha. \quad (3)$$

The covariant derivative is defined by

$$iD_i^\mu = i\partial^\mu - g_\omega^i \omega^\mu - \frac{g_\rho^i}{2} \vec{\tau} \cdot \vec{\rho}^\mu, \quad (4)$$

and the effective mass of nucleon is expressed as

$$M^* = m - g_\sigma \sigma, \quad (5)$$

where g_σ , g_ω , and g_ρ are coupling constants of σ , ω , and ρ mesons with nucleons, respectively; m is nucleon rest mass in vacuum which is taken to be $m = 939 \text{ MeV}$. It should be noted that here neutrons and protons are assumed to have the same mass in vacuum, but for astrophysical applications of nuclear matter EOS, the experimental masses of neutrons (m_n) and protons (m_p) should be adopted for accuracy and this contributes a linear splitting term in the isospin dependence of nucleon mass. The behavior that α particles dissolve at higher density can be described by introducing the in-medium effect. The in-medium binding energy of α -particle B_α is related to the α -particle effective mass M_α^* via the following relation:

$$M_\alpha^* = 4m - B_\alpha - g_\sigma^\alpha \sigma. \quad (6)$$

The meson Lagrangian densities are given by $\mathcal{L}_{\text{meson}} = \mathcal{L}_\sigma + \mathcal{L}_\omega + \mathcal{L}_\rho + \mathcal{L}_{\omega\rho}$ with

$$\mathcal{L}_\sigma = \frac{1}{2}\partial_\mu\sigma\partial^\mu\sigma - \frac{1}{2}m_\sigma^2\sigma^2 - \frac{1}{3}g_2\sigma^3 - \frac{1}{4}g_3\sigma^4, \quad (7)$$

$$\mathcal{L}_\omega = -\frac{1}{4}W_{\mu\nu}W^{\mu\nu} + \frac{1}{2}m_\omega^2\omega_\mu\omega^\mu + \frac{1}{4}c_3(\omega_\mu\omega^\mu)^2, \quad (8)$$

$$\mathcal{L}_\rho = -\frac{1}{4}\vec{R}_{\mu\nu}\cdot\vec{R}^{\mu\nu} + \frac{1}{2}m_\rho^2\vec{\rho}_\mu\cdot\vec{\rho}^\mu, \quad (9)$$

$$\mathcal{L}_{\omega\rho} = \Lambda_v(g_\omega^2\omega_\mu\omega^\mu)(g_\rho^2\vec{\rho}_\mu\cdot\vec{\rho}^\mu). \quad (10)$$

where $W^{\mu\nu}$ and $\vec{R}^{\mu\nu}$ are the antisymmetric field tensors for ω^μ and $\vec{\rho}^\mu$, respectively. In the RMF approach, meson fields are treated as classical fields and the field operators are replaced by their expectation values. For homogeneous matter, the nonvanishing expectation values of meson fields are $\sigma = \langle\sigma\rangle$, $\omega = \langle\omega^0\rangle$, and $\rho = \langle\rho_0^3\rangle$. Noting that the cluster binding energy is density dependent, one can express the equations of motion for the meson fields as

$$m_\sigma^2\sigma + g_2\sigma^2 + g_3\sigma^3 = \sum_{i=p,n,\alpha} g_\sigma^i n_i^s, \quad (11)$$

$$m_\omega^2\omega + c_3\omega^3 + 2\Lambda_v g_\omega^2 g_\rho^2 \omega \rho^2 = \sum_{i=p,n,\alpha} g_\omega^i n_i - \frac{m_\omega^2}{2g_\omega} \left(\frac{\partial \Delta B_\alpha}{\partial n_p^{\text{ps}}} + \frac{\partial \Delta B_\alpha}{\partial n_n^{\text{ps}}} \right) n_\alpha^s, \quad (12)$$

$$m_\rho^2\rho + 2\Lambda_v g_\omega^2 g_\rho^2 \omega^2 \rho = \sum_{i=p,n} g_\rho^i I_3^i n_i - \frac{m_\rho^2}{g_\rho} \left(\frac{\partial \Delta B_\alpha}{\partial n_p^{\text{ps}}} - \frac{\partial \Delta B_\alpha}{\partial n_n^{\text{ps}}} \right) n_\alpha^s, \quad (13)$$

where n_i^s is the scalar density, n_i is the vector density, ΔB_α represents the binding energy shift of the α particle, isospin I_3^i is equal to 1/2 for $i = p$ and -1/2 for $i = n$, and following Refs. [2,3,52], the meson- α couplings are assumed to have the following forms:

$$g_\sigma^\alpha = 4g_\sigma, \quad g_\omega^\alpha = 4g_\omega. \quad (14)$$

We note that some other forms for meson- α couplings are proposed in the literature [24,45–47].

The in-medium cluster binding energy $B_\alpha = B_\alpha^0 + \Delta B_\alpha$ is dependent on temperature T , total proton number density n_p^{tot} , and total neutron number density n_n^{tot} of the nuclear matter system, where B_α^0 is the binding energy for α particles in vacuum and its value is $B_\alpha^0 = 28.29566$ MeV [63]. The total energy shift of a cluster in nuclear medium mainly includes the self-energy shift, the Coulomb shift, and the Pauli shift. The gNL-RMF model has already contained the self-energy shift. The Coulomb shift can be obtained from the Wigner-Seitz approximation, and it is very small for the α particle considered here and thus is neglected in the present work. The Pauli shift can be evaluated in the perturbation theory with Gaussian approaches for α particles [2]. The energy shift ΔB_α is thus from the Pauli shift and it is assumed to have the

following empirical quadratic form [2], i.e.,

$$\Delta B_\alpha(n_p^{\text{tot}}, n_n^{\text{tot}}, T) = -\tilde{n}_\alpha \left[1 + \frac{\tilde{n}_\alpha}{2\tilde{n}_\alpha^0} \right] \delta B_\alpha(T), \quad (15)$$

where \tilde{n}_α stands for

$$\tilde{n}_\alpha = n_p^{\text{tot}} + n_n^{\text{tot}}, \quad (16)$$

and the density scale for α particles is given by

$$\tilde{n}_\alpha^0(T) = \frac{B_\alpha^0}{\delta B_\alpha(T)}. \quad (17)$$

The temperature dependence comes from $\delta B_\alpha(T)$, which is defined by [2]

$$\delta B_\alpha(T) = \frac{a_{\alpha,1}}{(T + a_{\alpha,2})^{3/2}}. \quad (18)$$

At a certain temperature, the Mott density of the α particles is obtained when the α -particle binding energy vanishes. In our previous work [52], the values of $a_{\alpha,1} = 137\,330$ MeV^{5/2} fm³ and $a_{\alpha,2} = 10.6701$ MeV are obtained by fitting the experimental Mott density [62], and we also use these values in the present work.

In the above derivations, to avoid complications due to the total baryon density dependence of the cluster binding energies in the present theoretical framework, following the work of Typel *et al.* [2], the dependence on the total baryon density in Eq. (15) is replaced by a dependence on the pseudodensities which are defined by

$$n_n^{\text{ps}} = \frac{1}{2}[\rho_\omega - \rho_\rho], \quad n_p^{\text{ps}} = \frac{1}{2}[\rho_\omega + \rho_\rho], \quad (19)$$

with

$$\rho_\omega = \frac{m_\omega^2}{g_\omega} \sqrt{\omega^\mu \omega_\mu}, \quad \rho_\rho = \frac{2m_\rho^2}{g_\rho} \sqrt{\vec{\rho}^\mu \vec{\rho}_\mu}. \quad (20)$$

The clusters are treated as pointlike particles, and the vector and scalar densities of the fermions ($i = p, n$) are given, respectively, by

$$n_i = 2 \int \frac{d^3k}{(2\pi)^3} [f_i^+(k) - f_i^-(k)], \quad (21)$$

$$n_i^s = 2 \int \frac{d^3k}{(2\pi)^3} \frac{M_i^*}{\sqrt{k^2 + M_i^{*2}}} [f_i^+(k) + f_i^-(k)], \quad (22)$$

with the occupation probability given by the Fermi-Dirac distribution, i.e.,

$$f_i^\pm = \frac{1}{1 + \exp\left[\left(\sqrt{k^2 + M_i^{*2}} \mp v_i\right)/T\right]}. \quad (23)$$

The densities of the α particles are obtained from

$$n_\alpha = \int \frac{d^3k}{(2\pi)^3} [b_\alpha^+(k) - b_\alpha^-(k)] + n_{\text{BEC}}, \quad (24)$$

$$n_\alpha^s = \int \frac{d^3k}{(2\pi)^3} \frac{M_\alpha^*}{\sqrt{k^2 + M_\alpha^{*2}}} [b_\alpha^+(k) + b_\alpha^-(k)] + n_{\text{BEC}}^s, \quad (25)$$

where n_{BEC} and n_{BEC}^s are the vector and scalar density of the α particles in the BEC state, respectively. It should be noted

that in homogeneous and isotropic matter n_{BEC} and n_{BEC}^s are actually identical. The Bose-Einstein distribution gives the occupation probability in the following form:

$$b_{\alpha}^{\pm} = \frac{1}{-1 + \exp[(\sqrt{k^2 + M_{\alpha}^{*2}} \mp v_{\alpha})/T]}. \quad (26)$$

For a system including nucleons and α particles in chemical equilibrium, as we are considering in the present work, v_i and v_{α} are the effective chemical potentials which are defined as $v_i = \mu_i - g_{\omega}^i \omega - g_{\rho}^i I_3^i \rho$ for nucleons and $v_{\alpha} = \mu_{\alpha} - 4g_{\omega} \omega$ for α particles, respectively. The chemical potential of the α particle is determined by

$$\mu_{\alpha} = 2\mu_n + 2\mu_p. \quad (27)$$

The thermodynamic quantities of homogeneous matter are easily derived from the energy-momentum tensor. The energy density is given by

$$\begin{aligned} \epsilon = & \sum_{i=p,n} 2 \int \frac{d^3k}{(2\pi)^3} \sqrt{k^2 + M_i^{*2}} (f_i^+ + f_i^-) \\ & + \int \frac{d^3k}{(2\pi)^3} \sqrt{k^2 + M_{\alpha}^{*2}} (b_{\alpha}^+ + b_{\alpha}^-) + n_{\text{BEC}} M_{\alpha}^* \\ & + \frac{1}{2} m_{\sigma}^2 \sigma^2 + \frac{1}{3} g_2 \sigma^3 + \frac{1}{4} g_3 \sigma^4 - \frac{1}{2} m_{\omega}^2 \omega^2 - \frac{1}{4} c_3 \omega^4 \\ & - \frac{1}{2} m_{\rho}^2 \rho^2 + \sum_{i=p,n} (g_{\omega}^i \omega n_i + g_{\rho}^i \rho I_3^i n_i) + 4g_{\omega} \omega n_{\alpha} \\ & - \Lambda_v g_{\omega}^2 g_{\rho}^2 \omega^2 \rho^2, \end{aligned} \quad (28)$$

and the pressure is obtained as

$$\begin{aligned} p = & \frac{1}{3} \sum_{i=p,n} 2 \int \frac{d^3k}{(2\pi)^3} \frac{k^2}{\sqrt{k^2 + M_i^{*2}}} (f_i^+ + f_i^-) \\ & + \frac{1}{3} \int \frac{d^3k}{(2\pi)^3} \frac{k^2}{\sqrt{k^2 + M_{\alpha}^{*2}}} (b_{\alpha}^+ + b_{\alpha}^-) \\ & - \frac{1}{2} m_{\sigma}^2 \sigma^2 - \frac{1}{3} g_2 \sigma^3 - \frac{1}{4} g_3 \sigma^4 + \frac{1}{2} m_{\omega}^2 \omega^2 + \frac{1}{4} c_3 \omega^4 \\ & + \frac{1}{2} m_{\rho}^2 \rho^2 + \Lambda_v g_{\omega}^2 g_{\rho}^2 \omega^2 \rho^2. \end{aligned} \quad (29)$$

It should be noted that the condensed bosons do not contribute to the pressure but to the energy density. The entropy density is expressed as

$$\begin{aligned} s = & - \sum_{i=p,n} 2 \int \frac{d^3k}{(2\pi)^3} [f_i^+ \ln f_i^+ \\ & + (1 - f_i^+) \ln(1 - f_i^+) + f_i^- \ln f_i^- \\ & + (1 - f_i^-) \ln(1 - f_i^-)] - \int \frac{d^3k}{(2\pi)^3} \\ & \times [b_{\alpha}^+ \ln b_{\alpha}^+ - (1 + b_{\alpha}^+) \ln(1 + b_{\alpha}^+) \\ & + b_{\alpha}^- \ln b_{\alpha}^- - (1 + b_{\alpha}^-) \ln(1 + b_{\alpha}^-)]. \end{aligned} \quad (30)$$

These thermodynamic quantities satisfy the Hugenholtz-van Hove theorem, i.e.,

$$\epsilon = Ts - p + \sum_{i=p,n,\alpha} \mu_i n_i. \quad (31)$$

It is convenient to define the internal energy per baryon as

$$E_{\text{int}} = \epsilon/n_B - m, \quad (32)$$

and the free energy per baryon is given by

$$F = E_{\text{int}} - T \frac{s}{n_B}. \quad (33)$$

The α condensation cannot occur above the critical temperature. For a system with fixed temperature, density, and isospin asymmetry, the thermodynamically favored state can be obtained by minimizing the free energy per baryon with respect to five independent variables, i.e., σ , ω , ρ , μ_p , and μ_n . Below the critical temperature, the α condensation occurs, and the effective chemical potential of the α particle equals the effective mass of the α particle, leading to consequence that the μ_p and μ_n are not independent at a fixed density of n_{BEC} for the α -BEC. In this case, we can use n_{BEC} to replace one of the two variables μ_p and μ_n to minimize the free energy per baryon. For a uniform three-dimensional Bose gas consisting of noninteracting particles with no apparent internal degrees of freedom, the critical temperature for Bose-Einstein condensation can be expressed analytically as [64]

$$T_c^{\text{Ideal}} = \left(\frac{n_{\text{num}}}{\zeta(3/2)} \right)^{2/3} \frac{2\pi \hbar^2}{m_{\text{Boson}} k_B}, \quad (34)$$

where n_{num} is the number density, m_{Boson} is the boson rest mass, k_B is the Boltzmann constant, and ζ is the Riemann ζ function. It would be interesting to compare the T_c^{Ideal} to the corresponding critical temperature obtained from the gNL-RMF model.

III. RESULTS AND DISCUSSION

In our previous work [52], it is found that the clustering effects are essentially independent of the interactions among nucleons and light nuclei in low-density nuclear matter. In the present work, therefore, we choose only one parameter set of the NL-RMF model, namely, FSUGold [60], for the ten parameters m_{σ} , m_{ω} , m_{ρ} , g_{σ} , g_{ω} , g_{ρ} , g_2 , g_3 , c_3 , and Λ_v .

First, we investigate the composition of dilute nuclear matter including α particles at zero temperature by using the gNL-RMF model. At zero temperature, all of the α particles occupy the lowest energy state and form α -BEC. In addition, the α particle has largest binding energy among the considered light nuclei with $A \leq 4$. Moreover, in the gNL-RMF model, for the Mott density of the light nuclei d , t , h , and α in nuclear matter at zero temperature, the α particle has the largest value. Therefore, only nucleons and α -BEC are present in the zero-temperature dilute nuclear matter in the gNL-RMF model calculations. Figure 1 shows the fraction for nucleons and α particles in the α -BEC as a function of the total baryon density in a dilute nuclear matter system at zero temperature with isospin asymmetry $\delta = 0$, $\delta = 0.3$, and $\delta = 0.6$, respectively. In zero-temperature dilute nuclear matter, the

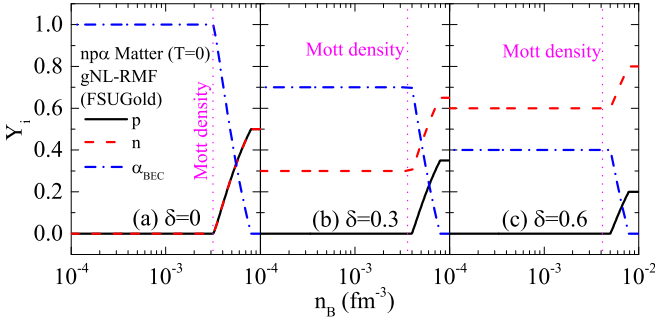


FIG. 1. The fraction for nucleons and α particles as a function of the total baryon density n_B in zero-temperature dilute nuclear matter with α condensation considered from the gNL-RMF model with FSUGold interaction for $\delta = 0$ (a), $\delta = 0.3$ (b), and $\delta = 0.6$ (c). The corresponding Mott density is also indicated.

fractions of neutrons, protons, and α particles in the α -BEC are simply determined by the n_p^{tot} and n_n^{tot} ($n_B = n_p^{\text{tot}} + n_n^{\text{tot}}$) as well as the in-medium α -particle binding energy, and all protons are bound in the α -BEC when the baryon density is below a critical density (denoted as dropping density n_{drop} above which the α -particle density starts to drop with density) whose value depends on the isospin asymmetry and is slightly larger than the corresponding Mott density ($\approx 3 \times 10^{-3} \text{ fm}^{-3}$) at which the α particles' binding energy vanishes. For the neutron-rich nuclear matter system, therefore, the system only contains neutrons and α -BEC when the baryon density is below the dropping density n_{drop} (i.e., $\approx 4 \times 10^{-3} \text{ fm}^{-3}$ for $\delta = 0.3$ and $\approx 5 \times 10^{-3} \text{ fm}^{-3}$ for $\delta = 0.6$), as observed in Figs. 1(b) and 1(c). It is interesting to see from Fig. 1(a) that the zero-temperature dilute symmetric nuclear matter ($\delta = 0$) becomes pure α matter in the α -BEC state when the baryon density is below the corresponding dropping density n_{drop} (which is very close to the Mott density for $\delta = 0$).

When the baryon density is larger than the Mott density of the α particle, the binding energy of α particles becomes negative and so the α particles are no longer in bound states, and in this case the α particles may be considered as effective resonance and continuum states. As the density further increases, the effective resonance and continuum states of α particles are expected to be continuously suppressed due to the negative binding energy (and the fraction of nucleons gradually increases to conserve the baryon number and isospin of the system) and eventually disappear at a transition density n_t above which the nuclear matter becomes pure nucleonic matter. Indeed, as expected, one sees from Fig. 1 that the fraction of α -BEC begins to decrease above the dropping density n_{drop} and then drops to zero at a critical density (i.e., the transition density n_t) around $\approx 8 \times 10^{-3} \text{ fm}^{-3}$, above which the system becomes pure nucleonic matter. The dropping density n_{drop} is slightly larger than the corresponding Mott density and this may be due to the interactions between the α particles and nucleons. (Note that the neutron density at n_{drop} is proportional to the isospin asymmetry.)

Shown in Fig. 2 is the internal energy per baryon as a function of the total baryon density in zero-temperature dilute nuclear matter with and without considering α condensation

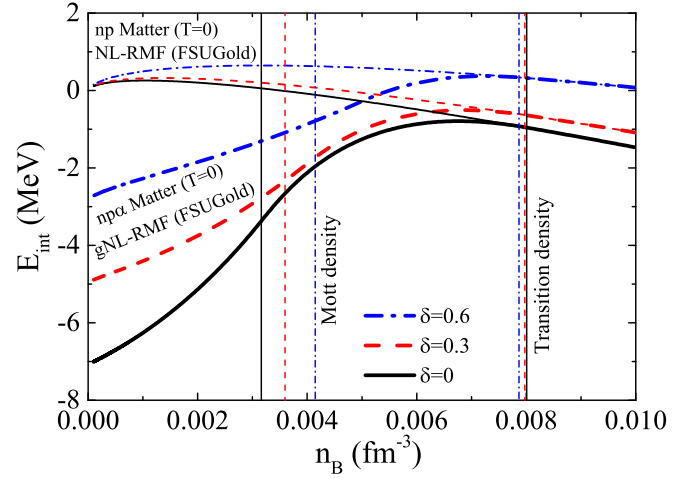


FIG. 2. The internal energy per baryon $E_{\text{int}}(n_B, \delta, T)$ as a function of the total baryon density n_B in zero-temperature dilute nuclear matter with (thick curves) and without (thin curves) considering α condensation from the gNL-RMF model with FSUGold interaction for $\delta = 0, 0.3$, and 0.6 . The corresponding Mott density and transition density are also indicated (thin vertical lines).

for isospin asymmetry $\delta = 0, 0.3$, and 0.6 . For both cases with and without considering α condensation, the internal energy per baryon at a fixed baryon density increases with the isospin asymmetry, and the increasing effect is much more pronounced in the case with α condensation considered than that without considering α condensation, especially at lower densities. Generally, the symmetric nuclear matter has the minimum internal energy per baryon. For a fixed isospin asymmetry, it is seen that the internal energy per baryon with and without considering α condensation is getting close to each other with increasing density and becomes identical above the transition density n_t , indicating the α clustering effects become weaker with increasing density. This feature is due to the fact that above the dropping density n_{drop} , the fraction of the α -BEC decreases with density and the α particles disappear above the transition density n_t , as shown in Fig. 1. Compared to the case without considering α condensation, the internal energy per baryon in the case with α condensation considered is drastically reduced by the formation of α particles.

For zero-temperature dilute symmetric nuclear matter with α condensation considered, the matter actually becomes pure- α matter as shown in Fig. 1(a). For pure- α matter, the interaction between α particles is ignorable when the density tends to zero and the internal energy per baryon is completely from the α -BEC. As a result, the internal energy per baryon of dilute symmetric nuclear matter at zero temperature approaches to the negative binding energy per baryon of the α particle in vacuum (i.e., $-B_\alpha^0 \approx -7.1 \text{ MeV}$) when the density tends to zero, which is indeed clearly seen in Fig. 2.

The clustering effects may break the empirical parabolic law for the isospin asymmetry dependence of nuclear matter EOS, especially at low temperatures [2–4,52]. It is thus interesting to check the empirical parabolic law for the dilute nuclear matter at zero temperature. To this end, we show in

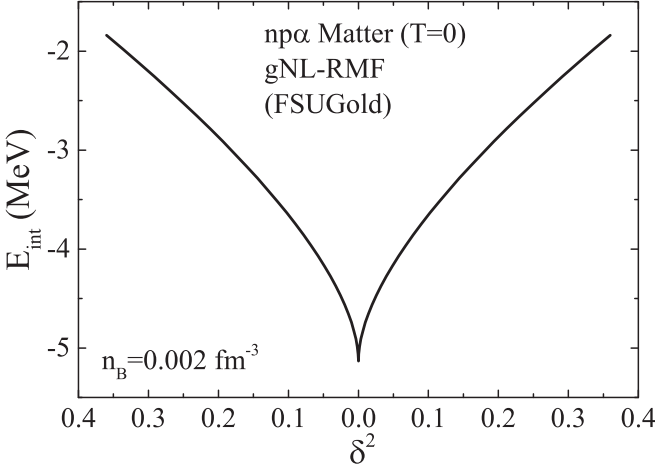


FIG. 3. The internal energy per baryon $E_{\text{int}}(n_B, \delta, T)$ vs squared isospin asymmetry δ^2 in zero-temperature dilute nuclear matter with α condensation considered at $n_B = 0.002 \text{ fm}^{-3}$ from the gNL-RMF model with FSUGold interaction.

Fig. 3 the internal energy per baryon $E_{\text{int}}(n_B, \delta, T = 0)$ as a function of the squared isospin asymmetry δ^2 in dilute nuclear matter at a representative density of $n_B = 0.002 \text{ fm}^{-3}$, which is below the Mott density of α particle in symmetric and asymmetric nuclear matter. (Note that the Mott density of the α particle in nuclear matter generally increases with the isospin asymmetry, as shown in Figs. 1 and 2.) As expected, the $E_{\text{int}}(n_B, \delta, T = 0)$ reaches its minimum value at $\delta = 0$. However, the curve significantly deviates from the linear relation $E_{\text{int}} \sim \delta^2$ around $\delta = 0$, indicating the violation of the empirical parabolic law. This can be understood from the fact that the formation of α -BEC significantly reduces the $E_{\text{int}}(n_B, \delta, T = 0)$ as seen in Fig. 2, and the system consists of only α -BEC and neutrons with their fractions linearly depending on the isospin asymmetry, as observed from Fig. 1 [see also Eqs. (38) and (39) in the following].

We now discuss the symmetry energy of dilute nuclear matter. Conventionally, the internal energy per baryon $E_{\text{int}}(n_B, \delta, T)$ of isospin asymmetric nuclear matter can be expanded in powers of isospin asymmetry $\delta = (n_n^{\text{tot}} - n_p^{\text{tot}})/(n_n^{\text{tot}} + n_p^{\text{tot}})$ as

$$E_{\text{int}}(n_B, \delta, T) = E_{\text{int}}(n_B, 0, T) + E_{\text{sym}}(n_B, T)\delta^2 + \dots, \quad (35)$$

where the density- and temperature-dependent symmetry (internal) energy E_{sym} is defined by

$$E_{\text{sym}}(n_B, T) = \frac{1}{2!} \left. \frac{\partial^2 E_{\text{int}}(n_B, \delta, T)}{\partial \delta^2} \right|_{\delta=0}. \quad (36)$$

On the other hand, under the parabolic approximation in which the higher order expansion coefficients (i.e., the high-order symmetry energies) on the right-hand side of Eq. (35) are assumed to be small and can be neglected, the symmetry energy can be obtained as

$$E_{\text{sym}}^{\text{para}}(n_B, T) = E_{\text{int}}(n_B, \delta = 1, T) - E_{\text{int}}(n_B, 0, T). \quad (37)$$

Within essentially all many-body theories to date, the parabolic approximation has been shown to be very success-

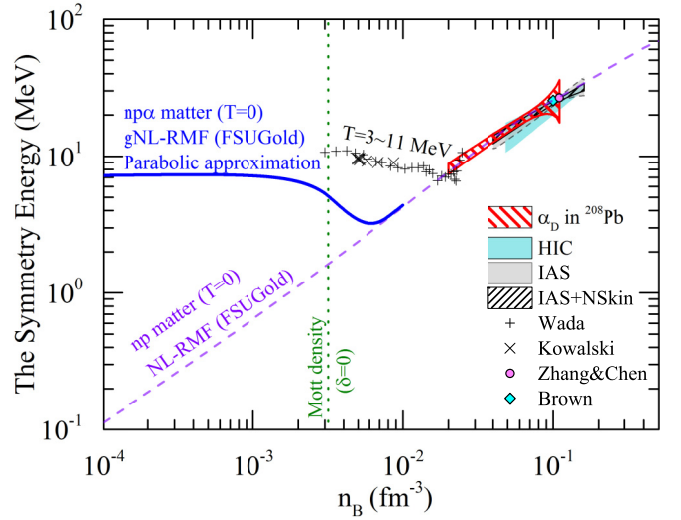


FIG. 4. The symmetry energy as a function of the total baryon density n_B in zero-temperature dilute nuclear matter with and without considering α condensation from the (g)NL-RMF model with FSUGold interaction. Some experimental constraints on the symmetry energy at zero-temperature are also included for comparison. The constraints on $E_{\text{sym}}^{\text{para}}(n_B, T)$ in the temperature range of $T \simeq 3\text{--}11 \text{ MeV}$ extracted from heavy-ion collisions (Wada and Kowalski) [66] are included only for exploratory comparison. See the text for details.

ful for nucleonic matter which only contains protons and neutrons, at least for densities up to moderate values (see, e.g., Ref. [65]). Therefore, usually we have $E_{\text{sym}}^{\text{para}}(n_B, T) \approx E_{\text{sym}}(n_B, T)$ for nucleonic matter. For dilute nuclear matter including light nuclei, especially at low densities ($\lesssim 0.02 \text{ fm}^{-3}$) and low temperatures ($\lesssim 3 \text{ MeV}$), as shown in Refs. [2,3,52]) as well as observed from the results presented above in this work, the higher order expansion coefficients on the right-hand side of Eq. (35) could be very large and thus the expansion of Eq. (35) may not be convergent, leading to not very meaningful symmetry energy with the conventional definition Eq. (36). Therefore, one usually uses the $E_{\text{sym}}^{\text{para}}(n_B, T)$ to define the symmetry energy for dilute nuclear matter including light nuclei and to compare with the experimental data (see, e.g., Refs. [2–4,52,66]). It should be noted that the $E_{\text{sym}}^{\text{para}}(n_B, T)$ is identical to the symmetry energy defined through the finite-difference formula $E_{\text{sym}}(n_B, T) = \frac{1}{2}[E_{\text{int}}(n_B, \delta = 1, T) - 2E_{\text{int}}(n_B, 0, T) + E_{\text{int}}(n_B, \delta = -1, T)]$ [2–4,66] if the mass difference between proton and neutron (as well as between h and t) is omitted. Similarly, one can define the symmetry free energy and the symmetry entropy in the same manner (see, e.g., Ref. [52]).

Figure 4 displays the symmetry energy $E_{\text{sym}}^{\text{para}}(n_B, T = 0)$ as a function of the total baryon density n_B in nuclear matter with and without considering α condensation from the (g)NL-RMF model with FSUGold interaction. For comparison, we also include some experimental constraints on the symmetry energy $E_{\text{sym}}(n_B, T = 0)$, i.e., the constraints from transport model analyses of midperipheral heavy-ion collisions of Sn isotopes (HIC) [67], the constraints from the SHF analyses

of isobaric analog states (IAS) as well as combining additionally the neutron skin “data” (IAS+NSkin) in Ref. [68], the constraints from analyzing the data on the electric dipole polarizability in ^{208}Pb (α_D in ^{208}Pb) [53], the constraints on the value of E_{sym} around $2/3n_0$ ($n_0 \approx 0.16 \text{ fm}^{-3}$ is nuclear saturation density) from binding energy difference between heavy isotope pairs [69] and properties of doubly magic nuclei [70], and the constraints on $E_{\text{sym}}^{\text{para}}(n_B, T)$ at densities below $0.2n_0$ and temperatures in the range 3–11 MeV from the analysis of cluster formation in heavy-ion collisions [66].

It is seen from Fig. 4 that compared to the results of pure nucleonic matter obtained from the NL-RMF calculations with FSUGold, the symmetry energy is drastically enhanced by including the α condensation in the gNL-RMF calculations. (Note that for nucleonic matter without light nuclei, one has $E_{\text{sym}}^{\text{para}}(n_B, T) \approx E_{\text{sym}}(n_B, T)$ in the NL-RMF calculations with FSUGold.) Very interestingly, one sees that the $E_{\text{sym}}^{\text{para}}(n_B, T = 0)$ in dilute nuclear matter with α condensation considered is saturated at about 7 MeV when the baryon density is very small (less than about $n_B = 10^{-3} \text{ fm}^{-3}$). It is constructive to examine such a saturation behavior in the low-density limit where analytic expressions might be obtained. According to Fig. 1, only α -BEC and neutrons can exist below the dropping density n_{drop} for the neutron-rich dilute nuclear matter, and the α -particle number density n_{BEC} in the BEC state and neutron number density n_n can be expressed as

$$n_{\text{BEC}} = n_B(1 - \delta)/4, \quad (38)$$

$$n_n = n_B\delta. \quad (39)$$

At zero temperature, the total energy density is given by

$$\epsilon = n_{\text{BEC}}M_\alpha^* + Cn_n^{5/3} + n_n m, \quad (40)$$

with $C = \frac{3}{5} \frac{\hbar^2}{2m} (3\pi^2)^{2/3} = 119.1 \text{ MeV fm}^2$. At very low densities so that one has $M_\alpha^* = 4m - B_\alpha - 4g_\sigma\sigma \approx M_\alpha$, the total energy per baryon can be expressed as

$$E = \frac{1}{4}M_\alpha + \left(m - \frac{M_\alpha}{4}\right)\delta + Cn_B^{2/3}\delta^{5/3}. \quad (41)$$

The second-order derivative of E with respect to δ is then obtained as

$$\frac{\partial^2 E}{\partial \delta^2} = \frac{10}{9}Cn_B^{2/3}\delta^{-1/3}. \quad (42)$$

Therefore, in the zero-temperature case for the dilute nuclear matter containing α -BEC and neutrons, the conventional definition of the symmetry energy E_{sym} [i.e., Eq. (36)] is divergent, and so one usually uses the symmetry energy definition $E_{\text{sym}}^{\text{para}}$ in the parabolic approximation [i.e., Eq. (37)]. From Eq. (41), one can obtain

$$E_{\text{sym}}^{\text{para}}(n_B, T = 0) = \left(m - \frac{M_\alpha}{4}\right) + Cn_B^{2/3}. \quad (43)$$

In the zero-density limit, one has

$$\begin{aligned} E_{\text{sym}}^{\text{para}}(n_B \rightarrow 0, T = 0) &= \left(m - \frac{M_\alpha}{4}\right) \\ &= B_\alpha^0/4 \approx 7.1 \text{ MeV}, \end{aligned} \quad (44)$$

and this is exactly what one has observed in Fig. 4. Above about $n_B = 10^{-3} \text{ fm}^{-3}$, the $E_{\text{sym}}^{\text{para}}(n_B, T = 0)$ in dilute nuclear matter with α -condensation considered decreases with density, and then increases after reaching a minimum value at a density of about $n_B = 6 \times 10^{-3} \text{ fm}^{-3}$, and eventually approaches to the $E_{\text{sym}}^{\text{para}}(n_B, T = 0)$ for nucleonic matter above the transition density ($\approx 8 \times 10^{-3} \text{ fm}^{-3}$).

It is nice to see from Fig. 4 that our present results on the $E_{\text{sym}}(n_B, T = 0)$ of nuclear matter from the gNL-RMF model with FSUGold are in good agreement with the constraints included in the figure for baryon density above $n_B = 0.02 \text{ fm}^{-3}$. Unfortunately, to the best of our knowledge, there currently have no experimental constraints on the $E_{\text{sym}}^{\text{para}}(n_B, T = 0)$ of dilute nuclear matter for baryon density below $n_B = 0.02 \text{ fm}^{-3}$. Our present results provide the predictions of the α -condensation effects on the symmetry energy in dilute nuclear matter at zero temperature and indicate that the $E_{\text{sym}}^{\text{para}}(n_B, T = 0)$ of nuclear matter is significantly enhanced due to the α condensation. We would like to point out that the constraints on $E_{\text{sym}}^{\text{para}}(n_B, T)$ in the density region of $n_B \simeq 0.003\text{--}0.03 \text{ fm}^{-3}$ and the temperature range of $T \simeq 3\text{--}11 \text{ MeV}$ extracted from heavy-ion collisions [66] are included in Fig. 4 only for exploratory comparison. For $n_B \simeq 0.003\text{--}0.03 \text{ fm}^{-3}$ and $T \simeq 3\text{--}11 \text{ MeV}$, there are no BEC in the nuclear matter and the clustering effects due to the formation of d , t , h , and α significantly enhance the $E_{\text{sym}}^{\text{para}}(n_B, T)$, leading to a reasonable agreement between the experimental data and the gNL-RMF model predictions as shown in Ref. [52]. In addition, one also sees a rather good agreement between the measured and calculated results in the quantum statistical (QS) approach that takes the formation of clusters into account (see, e.g., Refs. [4,66]). Therefore, any experimental or model-independent information on the symmetry energy of dilute nuclear matter at zero temperature for baryon density below $n_B = 0.02 \text{ fm}^{-3}$ is critically useful to confirm or disconfirm our present results based on the gNL-RMF model predictions.

Finally, we evaluate the critical temperature for α condensation in homogeneous dilute nuclear matter within the gNL-RMF model with the FSUGold interaction. The obtained results of the critical temperature T_c versus the total baryon density n_B in homogeneous dilute nuclear matter for $\delta = 0, 0.3$, and 0.6 are shown in Fig. 5. For comparison, we also include the critical temperature as a function of the total baryon density obtained from the analytical expression T_c^{Ideal} [i.e., Eq. (34)] for free α gas. It is seen that the critical temperature in the homogeneous dilute symmetric nuclear matter ($\delta = 0$) within the gNL-RMF model is almost identical to that in the free α gas when the baryon density is less than the corresponding α -Mott density (indicated by dotted lines in Fig. 5). This is because that in the gNL-RMF model for $\delta = 0$, the homogeneous dilute nuclear matter becomes pure α matter and the interactions between α particles are very weak at such low densities. In addition, the variation of the α -particle mass due to the binding energy shift in the homogeneous dilute nuclear matter is also very small compared with the rest mass of α particles in vacuum. When the baryon density is larger than the corresponding α -Mott density in the

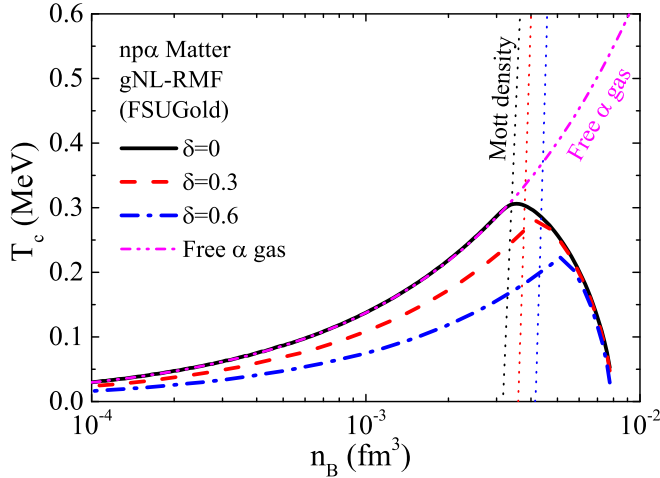


FIG. 5. The critical temperature T_c for α condensation as a function of the total baryon density n_B in dilute nuclear matter obtained from the gNL-RMF model with FSUGold interaction for $\delta = 0, 0.3$, and 0.6 . The corresponding Mott density is also indicated. For comparison, the critical temperature T_c^{ideal} for free α gas is also included.

homogeneous dilute symmetric nuclear matter, the fraction of α particles decreases with density, leading to the corresponding decreasing of the α -particle density and thus the critical temperature, and eventually the critical temperature vanishes at the transition density ($\approx 8 \times 10^{-3} \text{ fm}^{-3}$), as observed in Fig. 5.

Furthermore, one sees from Fig. 5 that the critical temperature depends on the isospin asymmetry of the nuclear matter system, and it decreases with the isospin asymmetry. This can be understood since for a fixed baryon density, the number density of α particles decreases with the isospin asymmetry [see, e.g., Eq. (38)] and thus the critical temperature also decreases with the isospin asymmetry due to the accordingly decreasing α -particle number density, as shown in Eq. (34). In addition, for isospin asymmetry $\delta = 0.3$ and 0.6 , the corresponding critical temperature exhibits similar density dependence as in the case of $\delta = 0$; namely, it increases with density, reaches a maximum value at a certain density, then decreases and vanishes at the transition density ($\approx 8 \times 10^{-3} \text{ fm}^{-3}$). It should be noted that the baryon density at the maximum critical temperature is slightly larger than the corresponding α -Mott density, and this may arise from the interactions between the α particles and nucleons, as also observed in Fig. 1 for the fraction of α -BEC in zero-temperature dilute nuclear matter.

Our results on the critical temperature for α condensation in homogeneous dilute symmetric nuclear matter below the α -Mott density within the gNL-RMF model are consistent with the results from the quasiparticle gas model obtained in Refs. [43,44] where the isospin dependence and the effects of resonance and continuum states above the Mott density are not considered. Generally speaking [64], the mean-field potentials in the gNL-RMF model can globally influence the

thermodynamic properties of the α matter but hardly affect the critical temperature for α condensation in homogeneous dilute nuclear matter. We would like to mention that, in the present calculations, the heavier nuclei are not considered, and only α particles and nucleons are taken into account. Including heavier nuclei, e.g., ^{56}Fe , may significantly influence the α condensation and the critical temperature, as shown in Ref. [44]. On the other hand, as pointed out in Ref. [44], in some situations (e.g., in heavy-ion collisions or at some stages of supernova explosions), the timescales of formation of heavier nuclei such as ^{56}Fe may be too long so that the light nuclei ($A \leq 4$) could be still the predominant component in the matter. In these situations, the α -BEC is expected to indeed occur in the clustered matter. In addition, it should be mentioned that the pairing effect, which is not considered in the present work, may become important for the Bose condensation at higher densities ($\gtrsim 3 \times 10^{-2} \text{ fm}^{-3}$) [49].

IV. CONCLUSION

We have investigated the thermodynamic properties of homogeneous dilute nuclear matter at zero temperature by using a generalized nonlinear relativistic mean-field (gNL-RMF) model. In the gNL-RMF model, the light nuclei d , t , h , and α are included as explicit degrees of freedom and treated as pointlike particles with their interactions described by meson exchanges and the in-medium effects on their binding energy are described by density- and temperature-dependent energy shifts with the parameters obtained by fitting the experimental Mott densities of the light nuclei extracted from heavy-ion collisions at Fermi energies.

Our results have shown that in homogeneous zero-temperature dilute nuclear matter, the binding energy of α particles is always larger than that of d , t , and h . As a result, the d , t , and h are not present in the system, and the homogeneous zero-temperature dilute nuclear matter is composed of nucleons and α particles. In particular, when the baryon density n_B is less than the dropping density ($\approx 3 \times 10^{-3} \text{ fm}^{-3}$), the zero-temperature symmetric nuclear matter is found to be in the state of pure α -BEC and the neutron-rich nuclear matter is composed of α -BEC and neutrons. Above the Mott density, the binding energy of α particles becomes negative and the resonance and continuum states may appear, which makes the fraction of the α particle begin to drop at the dropping density n_{drop} and eventually vanish at the transition density n_t .

In addition, we have explored the α -condensation effects on the symmetry energy of homogeneous dilute nuclear matter at zero temperature. We have shown that at zero temperature, the existence of the α -BEC in the homogeneous dilute nuclear matter violates the empirical parabolic law for the isospin asymmetry dependence of the nuclear matter equation of state and makes the conventional definition of the symmetry energy meaningless. Within the gNL-RMF model, the symmetry energy of the zero-temperature dilute nuclear matter defined under parabolic approximation is found to be drastically enhanced compared to the case without considering α -BEC, and it becomes saturated at about 7 MeV at very low densities ($\lesssim 10^{-3} \text{ fm}^{-3}$).

Finally, we have evaluated the critical temperature for α condensation in the homogeneous dilute nuclear matter. Our results indicate that the critical temperature increases with the baryon density up to the dropping density n_{drop} , then decreases, and eventually vanishes at the transition density n_t . In general, our results within the gNL-RMF model gives almost an identical critical temperature as that in the free α gas, indicating the α -particle interactions are not important in the homogeneous dilute nuclear matter, which is consistent with the result of the quasiparticle gas model.

ACKNOWLEDGMENTS

This work was supported in part by the National Natural Science Foundation of China under Grant No. 11625521, the Major State Basic Research Development Program (973 Program) in China under Contract No. 2015CB856904, the Program for Professor of Special Appointment (Eastern Scholar) at Shanghai Institutions of Higher Learning, Key Laboratory for Particle Physics, Astrophysics and Cosmology, Ministry of Education, China, and the Science and Technology Commission of Shanghai Municipality (No. 11DZ2260700).

-
- [1] G. Röpke, *Phys. Rev. C* **79**, 014002 (2009).
- [2] S. Typel, G. Röpke, T. Klähn, D. Blaschke, and H. H. Wolter, *Phys. Rev. C* **81**, 015803 (2010).
- [3] S. Typel, H. H. Wolter, G. Röpke, and D. Blaschke, *Eur. Phys. J. A* **50**, 17 (2014).
- [4] K. Hagel, J. B. Natowitz, and G. Röpke, *Eur. Phys. J. A* **50**, 39 (2014).
- [5] G. Giuliani, H. Zheng, and A. Bonasera, *Prog. Part. Nucl. Phys.* **76**, 116 (2014).
- [6] J. P. Ebran, E. Khan, T. Nikšić, and D. Vretenar, *Nature (London)* **487**, 341 (2012); *Phys. Rev. C* **87**, 044307 (2013); **89**, 031303(R) (2014); **90**, 054329 (2014).
- [7] B. Zhou, Y. Funaki, H. Horiuchi, Z. Ren, G. Röpke, P. Schuck, A. Tohsaki, C. Xu, and T. Yamada, *Phys. Rev. Lett.* **110**, 262501 (2013).
- [8] Z. H. Yang, Y. L. Ye, Z. H. Li, J. L. Lou, J. S. Wang, D. X. Jiang, Y. C. Ge, Q. T. Li, H. Hua, X. Q. Li *et al.*, *Phys. Rev. Lett.* **112**, 162501 (2014).
- [9] W. B. He, Y. G. Ma, X. G. Cao, X. Z. Cai, and G. Q. Zhang, *Phys. Rev. Lett.* **113**, 032506 (2014).
- [10] F. Aymard, F. Gulminelli, and J. Margueron, *Phys. Rev. C* **89**, 065807 (2014).
- [11] A. Tohsaki, H. Horiuchi, P. Schuck, and G. Röpke, *Rev. Mod. Phys.* **89**, 011002 (2017).
- [12] L. W. Chen, C. M. Ko, and B. A. Li, *Phys. Rev. C* **68**, 017601 (2003); *Nucl. Phys. A* **729**, 809 (2003); *Phys. Rev. C* **69**, 054606 (2004).
- [13] T. Gaitanos, M. Di Toro, S. Typel, V. Baran, C. Fuchs, V. Greco, and H. H. Wolter, *Nucl. Phys. A* **732**, 24 (2004).
- [14] Y. X. Zhang, Z. X. Li, C. S. Zhou, and M. B. Tsang, *Phys. Rev. C* **85**, 051602(R) (2012).
- [15] G. Röpke, S. Shlomo, A. Bonasera, J. B. Natowitz, S. J. Yennello, A. B. McIntosh, J. Mabilia, L. Qin, S. Kowalski, K. Hagel *et al.*, *Phys. Rev. C* **88**, 024609 (2013).
- [16] M. Hempel, K. Hagel, J. Natowitz, G. Röpke, and S. Typel, *Phys. Rev. C* **91**, 045805 (2015).
- [17] X. G. Cao, E. J. Kim, K. Schmidt, K. Hagel, M. Barbui, J. Gauthier, S. Wuenschel, G. Giuliani, M. R. D. Rodriguez, S. Kowalski *et al.*, *Phys. Rev. C* **99**, 014606 (2019).
- [18] T. Fischer, M. Hempel, I. Sagert, Y. Suwa, and J. Schaffner-Bielich, *Eur. Phys. J. A* **50**, 46 (2014).
- [19] S. Furusawa, K. Sumiyoshi, S. Yamada, and H. Suzuki, *Nucl. Phys. A* **957**, 188 (2017).
- [20] F. J. Fattoyev and J. Piekarewicz, *Phys. Rev. C* **82**, 025810 (2010).
- [21] B. K. Sharma and S. Pal, *Phys. Rev. C* **82**, 055802 (2010).
- [22] S. S. Avancini, C. C. Barros, Jr., L. Brito, S. Chiacchiera, D. P. Menezes, and C. Providência, *Phys. Rev. C* **85**, 035806 (2012).
- [23] A. R. Raduta, F. Aymard, and F. Gulminelli, *Eur. Phys. J. A* **50**, 24 (2014).
- [24] S. S. Avancini, M. Ferreira, H. Pais, C. Providência, and G. Röpke, *Phys. Rev. C* **95**, 045804 (2017).
- [25] A. Tohsaki, H. Horiuchi, P. Schuck, and G. Röpke, *Phys. Rev. Lett.* **87**, 192501 (2001).
- [26] S. Ohkubo and Y. Hirabayashi, *Phys. Rev. C* **70**, 041602(R) (2004).
- [27] M. Chernykh, H. Feldmeier, T. Neff, P. von Neumann-Cosel, and A. Richter, *Phys. Rev. Lett.* **98**, 032501 (2007).
- [28] T. Wakasa, E. Ihara, K. Fujita, Y. Funaki, K. Hatanaka, H. Horiuchi, M. Itoh, J. Kamiya, G. Röpke, H. Sakaguchi *et al.*, *Phys. Lett. B* **653**, 173 (2007).
- [29] P. Schuck, Y. Funaki, H. Horiuchi, G. Röpke, A. Tohsaki, and T. Yamada, *Prog. Part. Nucl. Phys.* **59**, 285 (2007).
- [30] Y. Funaki, H. Horiuchi, G. Röpke, P. Schuck, A. Tohsaki, and T. Yamada, *Nucl. Phys. News* **17**, 11 (2007); *Phys. Rev. C* **77**, 064312 (2008).
- [31] Y. Funaki, T. Yamada, H. Horiuchi, G. Röpke, P. Schuck, and A. Tohsaki, *Phys. Rev. Lett.* **101**, 082502 (2008).
- [32] S. Typel, *J. Phys.: Conf. Ser.* **420**, 012078 (2013).
- [33] S. Typel, *Phys. Rev. C* **89**, 064321 (2014).
- [34] G. Röpke, M. Schmidt, and H. Schulz, *Nucl. Phys. A* **424**, 594 (1984).
- [35] P. Nozières and S. Schmitt-Rink, *J. Low Temp. Phys.* **59**, 195 (1985).
- [36] M. Schmidt, G. Röpke, and H. Schulz, *Ann. Phys.* **202**, 57 (1990).
- [37] H. Stein, A. Schnell, T. Aim, and G. Röpke, *Z. Phys. A* **351**, 295 (1995).
- [38] M. Beyer, S. A. Sofianos, C. Kuhrt, G. Röpke, and P. Schuck, *Phys. Lett. B* **488**, 247 (2000).
- [39] J. M. Lattimer and F. D. Swesty, *Nucl. Phys. A* **535**, 331 (1991).
- [40] H. Shen, H. Toki, K. Oyamatsu, and K. Sumiyoshi, *Astrophys. J. Suppl.* **197**, 20 (2011).
- [41] C. J. Horowitz and A. Schwenk, *Phys. Lett. B* **642**, 326 (2006); *Nucl. Phys. A* **776**, 55 (2006).
- [42] S. Mallik, J. N. De, S. K. Samaddar, and S. Sarkar, *Phys. Rev. C* **77**, 032201(R) (2008).
- [43] S. Heckel, P. P. Schneider, and A. Sedrakian, *Phys. Rev. C* **80**, 015805 (2009).
- [44] X. H. Wu, S. B. Wang, A. Sedrakian, and G. Röpke, *J. Low Temp. Phys.* **189**, 133 (2017).
- [45] M. Ferreira and C. Providência, *Phys. Rev. C* **85**, 055811 (2012).

- [46] H. Pais, F. Gulminelli, C. Providência, and G. Röpke, *Phys. Rev. C* **97**, 045805 (2018).
- [47] H. Pais, F. Gulminelli, C. Providência, and G. Röpke, *Phys. Rev. C* **99**, 055806 (2019).
- [48] Ş. Mişicu, I. N. Mishustin, and W. Greiner, *J. Phys. G* **42**, 075104 (2015).
- [49] G. Röpke, A. Schnell, P. Schuck, and P. Nozières, *Phys. Rev. Lett.* **80**, 3177 (1998).
- [50] T. Sogo, R. Lazauskas, G. Röpke, and P. Schuck, *Phys. Rev. C* **79**, 051301(R) (2009).
- [51] T. Sogo, G. Röpke, and P. Schuck, *Phys. Rev. C* **82**, 034322 (2010).
- [52] Z. W. Zhang and L. W. Chen, *Phys. Rev. C* **95**, 064330 (2017).
- [53] Z. Zhang and L. W. Chen, *Phys. Rev. C* **92**, 031301(R) (2015).
- [54] J. D. Walecka, *Ann. Phys. (NY)* **83**, 491 (1974).
- [55] J. Boguta and A. R. Bodmer, *Nucl. Phys. A* **292**, 413 (1977).
- [56] H. Müller and B. D. Serot, *Nucl. Phys. A* **606**, 508 (1996).
- [57] S. Kubis and M. Kutschera, *Phys. Lett. B* **399**, 191 (1997).
- [58] B. Liu, V. Greco, V. Baran, M. Colonna, and M. Di Toro, *Phys. Rev. C* **65**, 045201 (2002).
- [59] C. J. Horowitz and J. Piekarewicz, *Phys. Rev. Lett.* **86**, 5647 (2001).
- [60] B. G. Todd-Rutel and J. Piekarewicz, *Phys. Rev. Lett.* **95**, 122501 (2005).
- [61] L. W. Chen, C. M. Ko, and B. A. Li, *Phys. Rev. C* **76**, 054316 (2007).
- [62] K. Hagel, R. Wada, L. Qin, J. B. Natowitz, S. Shlomo, A. Bonasera, G. Röpke, S. Typel, Z. Chen, M. Huang *et al.*, *Phys. Rev. Lett.* **108**, 062702 (2012).
- [63] M. Wang, G. Audi, F. G. Kondev, W. J. Huang, S. Naimi, and X. Xu, *Chin. Phys. C* **41**, 030003 (2017).
- [64] K. Huang, *Statistical Mechanics*, 2nd ed. (Wiley, New York, 1987).
- [65] B. A. Li, L. W. Chen, and C. M. Ko, *Phys. Rep.* **464**, 113 (2008).
- [66] J. B. Natowitz, G. Röpke, S. Typel, D. Blaschke, A. Bonasera, K. Hagel, T. Klähn, S. Kowalski, L. Qin, S. Shlomo *et al.*, *Phys. Rev. Lett.* **104**, 202501 (2010); S. Kowalski, J. B. Natowitz, S. Shlomo, R. Wada, K. Hagel, J. Wang, T. Materna, Z. Chen, Y. G. Ma, L. Qin *et al.*, *Phys. Rev. C* **75**, 014601 (2007); R. Wada, K. Hagel, L. Qin, J. B. Natowitz, Y. G. Ma, G. Röpke, S. Shlomo, A. Bonasera, S. Typel, Z. Chen *et al.*, *ibid.* **85**, 064618 (2012).
- [67] M. B. Tsang, Y. Zhang, P. Danielewicz, M. Famiano, Z. Li, W. G. Lynch, and A. W. Steiner, *Phys. Rev. Lett.* **102**, 122701 (2009).
- [68] P. Danielewicz and J. Lee, *Nucl. Phys. A* **922**, 1 (2014).
- [69] Z. Zhang and L. W. Chen, *Phys. Lett. B* **726**, 234 (2013).
- [70] B. A. Brown, *Phys. Rev. Lett.* **111**, 232502 (2013).